1

AFF-1 fusogen can rejuvenate the regenerative potential of adult dendritic trees via self-fusion

4

5   Veronika Kravtsov[1,#], Meital Oren-Suissa[1,2,#], and Benjamin Podbilewicz[1†]

6

7   [1]Department of Biology, Technion- Israel Institute of Technology, Haifa 32000, Israel

8   [#]These authors contributed equally to this work

9   [†]Correspondence to: podbilew@technion.ac.il

10 Additional footnotes:

11 [2]Present address: Columbia University Medical Center, Department of Biochemistry &

12 Molecular Biophysics, New York, 10032, USA

13

14 **Short title:** Cell fusion proteins act as neuronal anti-aging molecules in *C. elegans*

15

16   **Abstract**

17   The aging brain undergoes structural changes, affecting brain homeostasis, neuronal function

18   and consequently cognition. Neuronal dendrites are central in the formation and maintenance

19   of neural networks, and the extent of arborization determines the synaptic properties of the

20   neuron. The complex architecture of dendritic arbors poses a challenge to understanding age-

21   dependent morphological alterations, behavioral plasticity and remodeling following brain

22   injury. Here, we use the PVD polymodal neurons of *C. elegans* as a model to study how

23   aging affects neuronal plasticity. Using confocal live imaging of *C. elegans* PVD neurons, we

24   demonstrate major age-related progressive morphological alterations of intricate dendritic

25   arbors. We show that insulin/IGF-1 receptor mutations (*daf-2*) fail to inhibit the progressive

26   morphological aging of dendrites and do not prevent the minor, but significant, decline in

27   response to harsh touch during aging. We use the PVD neurons to study how aging animals

28   respond to neuronal trauma. We uncovered that PVD aging is characterized by a major

29   decline in regenerative potential of dendrites following experimental laser dendrotomy.

30   Furthermore, the remodeling of transected dendritic trees via AFF-1-mediated self-fusion can

31   be restored in old animals by DAF-2 insulin/IGF-1 receptor mutations, and can be

32   differentially reestablished by ectopic expression of AFF-1 fusion protein (fusogen). Thus,

33   AFF-1 fusogen ectopically expressed in the PVD and mutations in DAF-2/IGF-1R,

34   differentially rejuvenate some aspects of dendritic regeneration following injury.

35

Introduction

Aging is the primary risk for neuronal diseases and general cognitive decline in humans [1], yet, our understanding of the process of neuronal aging at the molecular and cell biological levels is still limited. In particular, very few studies have investigated the fate of complex dendritic arbors during aging, and their regenerative capacity following brain injury or trauma. Signaling via the DAF-2 Insulin/IGF-1 receptor is the most prominent and conserved pathway that controls aging and longevity of *C. elegans*, flies, and mammals [2]. *C. elegans* is a powerful system to study the genetics of neuronal aging and regeneration [2-4]. Normally, when the DAF-2/IGF-1 receptor is activated it induces a conserved PI3K/AKT kinase cascade, which in turn inhibits the DAF-16/FOXO transcription factor from entering into the nucleus. Reduction of *daf-2* function doubles life span, and long-lived worms are considered to stay healthy for longer [2,5]. In these animals, DAF-16/FOXO affects transcription of different genes that encode heat-shock proteins, antimicrobial proteins, antioxidants, and other molecules, which leads ultimately to extended lifespan [6,7]. Recently, aging-associated axonal morphological alterations and decline in regenerative capacity were described in *C. elegans*. *daf-2* mutations delayed these age-related morphological changes and improved regeneration of aged severed axons in a *daf-16*-dependent manner [8-11]. Moreover, in the case of GABA motor neurons, as adult animals age there is a reduction in axon growth, retraction and regrowth in response to injury. Surprisingly, the decline in regeneration by regrowth is controlled by *daf-16* in a cell-autonomously fashion and independently of lifespan [11].

The process of regeneration of injured axons in vertebrates and invertebrates often involves degeneration of the distal part followed by regrowth [12-14]. However, different invertebrates, including nematodes and crustaceans, use membrane fusion as an alternative mechanism for repair of injured axons [15-18]. Cell fusion events were also observed in the

3

61   brains of mammals both spontaneously and as a result of injury such as stroke [19-21], but the

62   role of these events has remained unclear [22]. In *C. elegans*, axonal regeneration via auto-

63   fusion is mediated by the fusogen EFF-1 [15,16,18]. EFF-1 is the first *bona fide* eukaryotic

64   developmental cell-cell fusion protein. It is expressed in different cell types including

65   neurons, and mediates fusion between cells by a homotypic mechanism [23-25]. Thus, EFF-1 has

66   to be expressed in both cellular membranes for them to merge and the high-resolution crystal

67   structure of EFF-1 ectodomain suggests that EFF-1 acts by a mechanism that is distinct from

68   viral-induced fusion. EFF-1, not only has to be present in both membranes for them to fuse, it

69   also appears to interact in trans forming complexes that tether and fuse the membranes [24,26].

70   We have been studying the role of fusion proteins in the PVD neuron, a polymodal

71   nociceptor that senses harsh touch to the body, cold temperature, and posture [27-30]. The PVD

72   neuron exhibits an elaborate and invariant dendritic structure, which is composed of a

73   repetitive unit that resembles a candelabrum (or a "menorah") **(Fig 1A)** [28]. These dendritic

74   trees arise and are dynamically maintained through several intrinsic and extrinsic genetic

75   pathways [28-38].

76   The PVD develops in a stereotypic fashion from the L2 larval stage to the young adult

77   [28]. The fusion protein EFF-1 mediates dendrite retraction and auto-fusion of excess branches

78   by a novel cell-autonomous pruning mechanism [28]. Thus, this fusogen maintains the

79   structural units by trimming excess branching during normal developmental arborization [28].

80   AFF-1, a paralog of EFF-1, is a second *C. elegans* fusogen displaying a more restricted tissue

81   distribution pattern [39]; AFF-1 was not found to be involved in PVD remodeling during

82   development [40]. AFF-1 and EFF-1 fusion proteins also auto-fuse epithelial and myoepithelial

83   cells to form tubes and reshape glial cells [41-44]. Moreover, it has recently been demonstrated

84   that in vertebrates auto-fusion takes place in the development of the vascular endothelium,

85   where it leads to pruning of excess blood vessels [45] in a process that remarkably resembles

86   EFF-1-mediated PVD pruning [28]. It is unknown whether PVD structure and function is

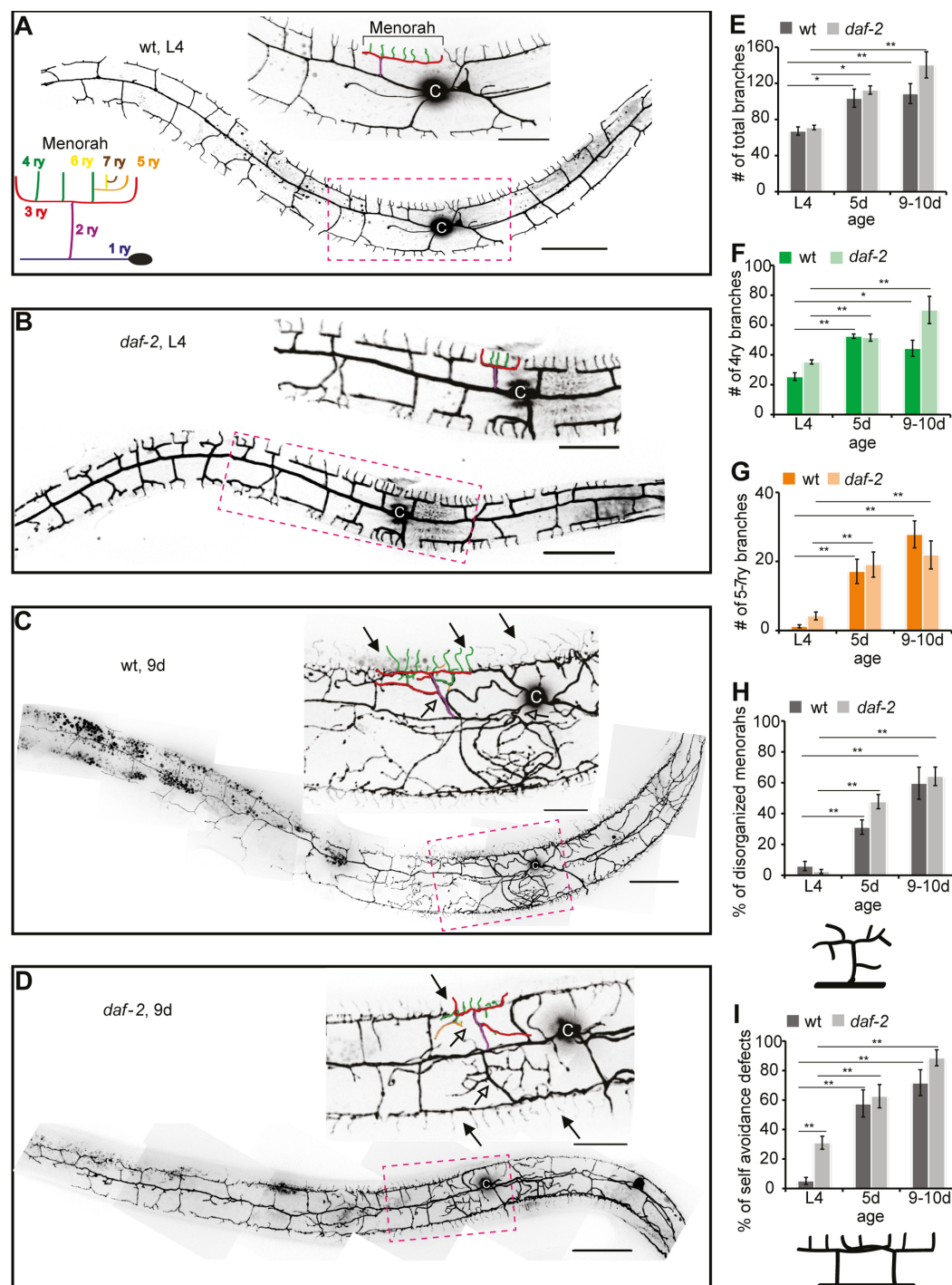87   affected by aging and by the activity of fusion proteins.

88
89
90   **Fig 1. PVD's dendritic alterations during aging**

91   **(A-D)** PVD in wild-type (wt; **A** and **C**) and *daf-2* mutants (**B** and **D**) at L4 stage and 9 days
92   of adulthood (9d). Upper panels, magnified boxed areas with candelabra-shaped units colored
93   according to the scheme (**A**). c, cell body. Scale bars, 50 μm and 20 μm in magnified images.
94   Anterior is left and ventral is down in all the figures. Filled arrows, self-avoidance defects.
95   Empty arrows, disorganized menorahs.

96   **(E-I)** Quantitation of phenotypes. Percentages were calculated for 100 μm of length around
97   the cell body. Error bars, ± s.e.m. Statistics were calculated using student's *t*-test, **P<0.01,*
98   ***P<0.001.* (**E**) There is no significant difference between wild-type animals and *daf-2*
99   mutant animals at any age (one-way ANOVA). However, there is a significant difference
100 between different developmental stages of the same genotype (*P<0.01 for wt and P<0.0001*
101 *for daf-2).).*(**F-G**) According to ANOVA age gives a significant difference in 4ry and in 5-
102 7ry branching number both in wt and in *daf-2* backgrounds (*P<0.001 for 4ry both wt and*
103 *daf-2*; 5-7ry branching *P<0.0001 for wild-type and P<0.001 for daf-2).*(**H-I**) According to
104 one-way ANOVA age has significance in menorahs disorganization and loss of self-
105 avoidance in both wild-type and *daf-2* (*P<0.0001 for wt and P< P<0.0001 for daf-2).*
106 Number of animals analyzed: *daf-2* n ≥ 8 and wild-types n ≥ 5.

107

108 Here, we show that induction of cellular fusion proteins (fusogens) can remodel and facilitate

109 regeneration of dendrites in polymodal PVD neurons of aging *Caenorhabditis elegans*. Using

110 whole-animal live imaging, we find that the PVD dendritic trees, composed of repetitive

111 orderly multibranched units, show age-dependent hyperbranching, disorganization, and loss

112 of self-avoidance. These processes, while independent of canonical lifespan-regulating

113 pathways, can be partially rescued by ectopic expression of the fusogen EFF-1 that prunes

114 multibranched dendrites. Surprisingly, most wild-type and *daf-2* (Insulin/IGF-1Receptor)

115 mutant adults that have disorganized dendritic trees have normal response to harsh touch.

116 Furthermore, we found a decreased capacity of old animals to repair laser-induced injured

117 dendrites via auto-fusion that can be restored by reducing DAF-2 function or by ectopic

118 expression of the EFF-1 paralog AFF-1 that remodels dendritic trees via merging of injured

119 branches. Our findings demonstrate that fusogens are sufficient to maintain the dendritic

120 arbor structure and increase its regeneration potential by auto-fusion in aging animals. These

121 antiaging strategies can be potentially applied to other organisms to help them recover from

122 stroke, brain trauma and spinal cord injury.

123

124

Results

Progressive dendritic remodeling during aging is independent from the Insulin/IGF-1 pathway

Aging neurons lose their ability to remodel following injury, change their complex morphology, and may degenerate [1]. Whereas axon degeneration during aging has been studied extensively both in mammals and in invertebrates, the fate of complex dendritic trees in old animals has not been studied in detail in any organism. To determine how aging affects the complex arborized dendritic structure, we analyzed the *C. elegans* PVD dendritic branching patterns from the fourth larval stage (L4) to ten-day-old adults. We found that during aging PVD's dendritic structures undergo disorganization and hyperbranching **(Figs 1A, 1C, and S1)**. Remarkably, we found that these age-dependent morphological changes of the PVD dendritic pattern were not affected in long-lived animals carrying a mutation in *daf-2* **(Figs 1A-1H, and S1)**. Adjacent PVD dendrites normally avoid each other [46], and we found that as the animal ages the structural units lose their self-avoidance properties **(Fig 1C, 1D, and 1I)**. Consistently, this age-dependent dendritic pattern did not improve in *daf-2* mutant animals; young *daf-2* animals at the L4 stage exhibited significantly more *daf-16*-dependent self-avoidance deficiencies in comparison to wild-type **(Fig 2)**. Thus, taken together our results reveal that during aging there is a *daf-2*-independent increase in disorganization of branching and loss of self-avoidance.
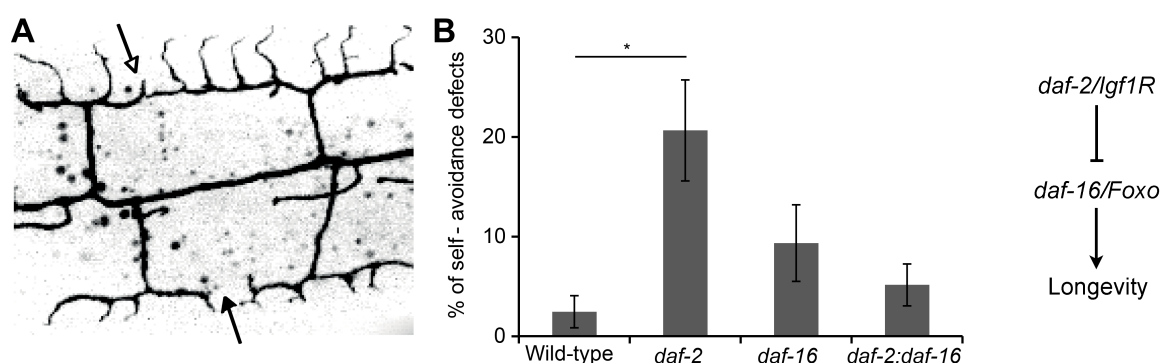

144

7

Fig 2. DAF-2-DAF-16 control self-avoidance at L4 stage

(A) Image showing four wild-type PVD dendritic units labeled with GFP, two of them do not overlap (filled arrow) and two show defective self-avoidance (empty arrow).

(B) Percentage of defects in self-avoidance in 100 μm of length around PVD cell body at L4 stage in different genotypes, n ≥ 7. Defective self-avoidance increases in *daf-2* mutants in a *daf-16*-dependent manner. Error bars are ± s.e.m. Statistics were calculated using ANOVA, followed by *t* test, * *P<0.05*.

The elaborate PVD structure is highly dynamic in young animals, exhibiting constant growth and retraction of individual high order branches [47-49]. To further understand the dynamics of the age-dependent dendritic tree remodeling, we followed individual animals over time and analyzed time-lapse movies. We found that 5-day adults still exhibited some plasticity of the dendritic tree, with dynamic growth and retraction events **(Fig 3A** and **Movie S1)**; however, both growth and retraction were two times slower **(Fig 3B)** compared to younger L4 animals, imaged under the same conditions. Next we quantified the number of movements of branches. Most branches showed dynamic movements ending either with elongation or with shortening, but a minority of branches only grew or only retracted throughout the movies. When young animals were imaged, not only the rates of growth and retraction were higher, but also the number of dynamic events involving both growth and retraction were higher (data not shown). Interestingly, both in L4 larvae and 5d adults there were more events that ended with outgrowth or elongation rather than retraction events. We also found that the decrease in dynamic events with age was proportional both for outgrowth and retraction. Thus, we conclude that at all ages there are slightly more growth events than retractions, which leads to branch accumulation with time and thus causing hyperbranched phenotype of the PVD. These experiments reveal that the PVD dendritic arbors grow and age in a dynamic way and not in a step-wise manner as apparent from still images. This dynamic growth and retraction together with the increase in branching as animals age suggest that hyperbranching is part of the normal dynamic growth of the dendritic arbors.
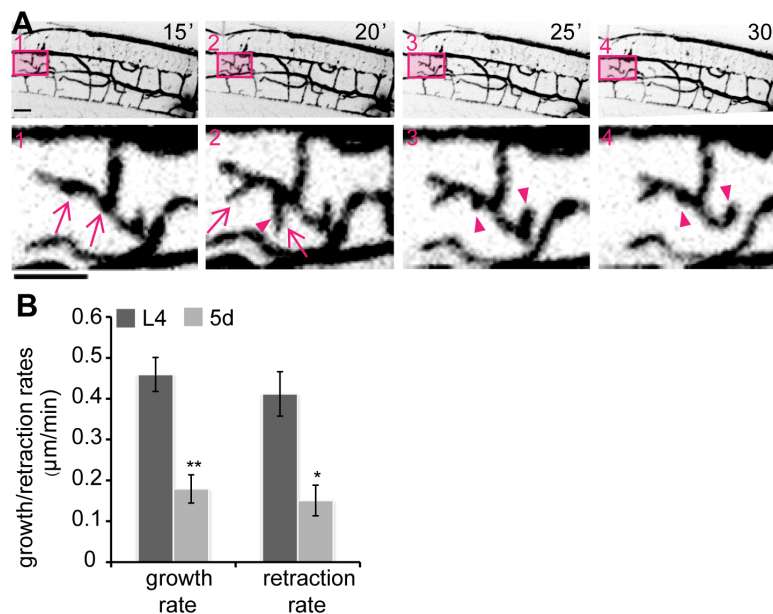
8

Fig 3. Adults show a reduction in dendritic plasticity

(A) Time-lapse confocal projections of 5 days of adulthood (5d) wild-type animal. Boxed areas are enlarged in the lower panel and reveal dynamic growth (arrows) and retraction (arrowheads) of branches. Scale bars, 10 μm.

(B) Growth and retraction rates in μm/minute of branches at L4 stage and 5d as measured from time-lapse movies. ≥ 18 branches were analyzed from 4 L4 animals and 2 5d animals. Error bars are ± s.e.m. *P* values from *t* tests: * *P<0.01*, ** *P<0.001*. See also **Movie S1**.

We speculated that reduced dendritic plasticity and structural changes in aged animals would affect the functionality of the PVD neurons. To shed more light on the link between structure and function of dendrites during aging, we performed a functionality test. PVD responds to harsh stimulations, and we used a classic harsh touch assay in *mec-4* mutant animals to specifically test PVD activity without the background light touch response mediated by the six light-touch mechanosensory neurons [28,50]. First, we found that although *mec-4* animals have shorter life span [10], their dendrites looked similar to wild-type between the ages L4-5d **(Fig 4)**, which further demonstrates that the morphological alterations we see are lifespan-independent. Second, we found that the PVD functionality showed a minor decrease with aging, with 5d adults presenting a small but significantly reduced harsh touch response in comparison to 1d adults, in both *mec-4* and *mec-4;daf-2* double mutants **(Fig 4F)**. We cannot rule out that multiple components of the sensorimotor circuit contribute to

192   the age-dependent decline in PVD activities. Thus, our results reveal that the morphological

193   and behavioral hallmarks of aging in PVD dendritic arbors are independent from the

194   canonical IGF-1 pathway that affects lifespan. Moreover, the fact that the dramatic increase

195   in branching and loss of self-avoidance in middle-aged animals (5d-adults; **Figs 1-3**)

196   correlates with lack of response to harsh touch in only 10% of the worms, compared to 1d

197   adults, suggests that hyperbranching, loss of self avoidance and disorganization of dendritic

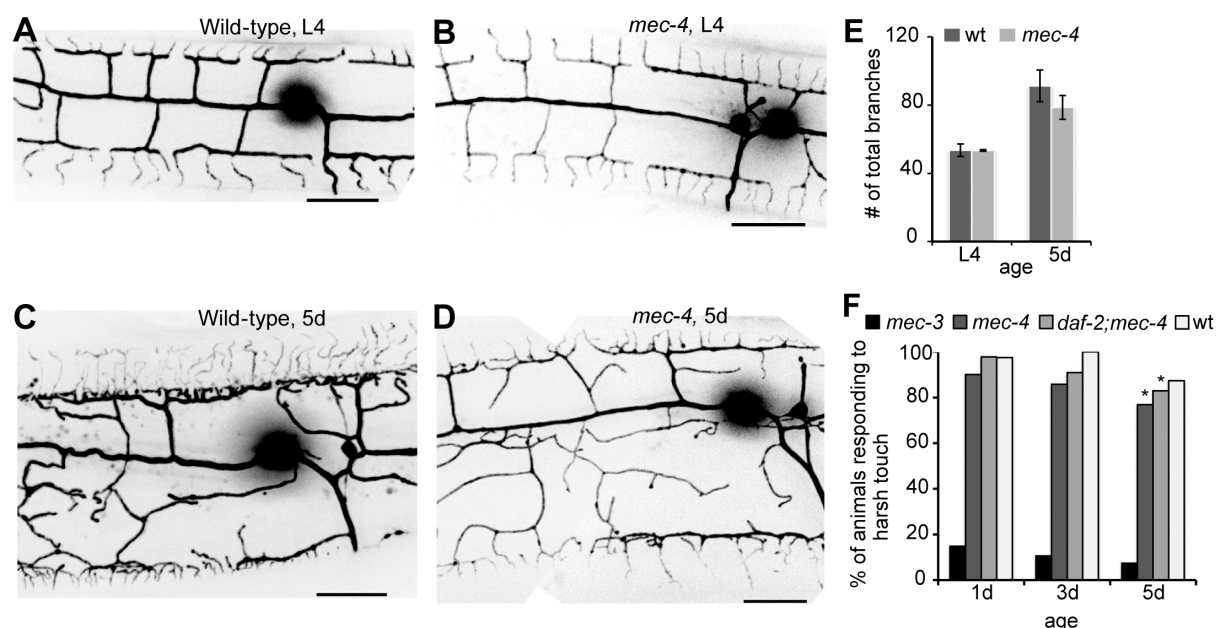198   trees might be normal and not deleterious for the behavioral response.

199

200   **Fig 4. Decline in response to harsh touch during aging in both wild-type and *daf-2***

201   **(A-D)** PVD's cell-body region of wt and light-touch insensitive *mec-4* mutants at the L4
202   stage and at 5 days of adulthood (5d). Scale bars are 20 μm.

203   **(E)** Total number of branches counted in 100 μm of length around cell-body in wt and *mec-4*
204   mutants at L4 and 5d (no significant differences between wt and *mec-4)*. Error bars are ±
205   s.e.m.

206   **(F)** Percentage of animals responding to harsh touch by escaping away from the stimulus. At
207   the age of 5d, the response declined in *mec-4* mutants and in *daf-2;mec-4* double mutants. *P*
208   values from χ2 test as compared between 1d to other ages (3d or 5d) for each genotype: * *P*
209   *<0.05*. Number of animals: *mec-3* ≥ 50; *mec-4* ≥ 70; *daf-2;mec-4* ≥ 40; wt ≥ 26.

210

211   In summary, the changes in dendritic architecture are not necessarily a deleterious aspect of

212   aging, but could actually be part of normal neuronal maintenance that keeps the cell

213   functioning over time. The fact that they are not altered in *daf-2* mutants supports this idea, as

214   does the functional data that shows most of the neurons function fine in 5 days adults (**Fig 4**).

215   Thus, the observed increase in dendrite branching and the disorganized appearance of the

216   trees is probably adaptive as the animals increase in girth.

217   **Age-dependent decline in dendrite regeneration is dependent on Insulin/IGF-1**

218   Mammalian axons regenerate better in younger individuals than in adults [51]. Similarly, axonal

219   regenerative ability declines drastically as nematodes advance through development and age

220   [11,52]. Our knowledge is still poor on the regenerative capacity of the dendrite, and how aging

221   affects this process of neuronal repair [53-55]. To study dendritic regeneration we severed the

222   primary dendrites of PVD neuron in aging adults. Typically, the PVDs show robust

223   regeneration at L4 larval stage, consisting in dendrite sprouting from the proximal fragment

224   still attached to the cell body and reconnection via fusion with the separated distal dendrite

225   fragment **(Fig 5A, Movie S2)**. To directly measure reconnection by auto-fusion, we used the

226   photoconvertible reporter Kaede **(Fig S2 and Movie S3)**. If fusion fails to occur, the

227   detached distal part eventually degenerates. We found that 2-3 day-old wild-type adults

228   respond more slowly to laser dendrotomy in comparison to L4 and young adults (~70% of the

229   young animals presented regeneration, whereas at the age of 2-3d neither regeneration nor

230   degeneration occurred within 3-6 hours (**Fig 5E and Movie S4)**. At the age of 5 days, the

231   ability to regenerate by dendrite auto-fusion was almost completely lost **(Fig 5C** and **5F)**.

232   Thus, we found that relatively young adults already show a decline in their dendritic

233   regenerative ability.

234   To determine whether the decline in the ability to remodel dendrites by auto-fusion is

235   dependent on the Insulin/IGF-1 pathway we tested whether the long-lived *daf-2* mutants are

236   prevented from losing their dendritic self-fusion ability. We found that *daf-2* mutants showed

237   similar regeneration to wild-type at L4 stage **(Fig 5B** and **5F)**, whereas at older age (5d) *daf-2*

238   mutants had a much higher regenerative ability than wild-types (70% successful regeneration

239   in *daf-2* versus 12.5% in wild-type) **(Fig 5D** and **5F)**. Similarly to axonal response to injury

240   [11], we found that DAF-2 inhibits regeneration of aged dendrites through inhibition of DAF-

241   16, as *daf-16* mutants and *daf-2;daf-16* double mutants showed regenerative decline during

242   aging similar to wild-type **(Fig 5F)**. In conclusion, our results reveal that dendrite

243   regeneration following transection declines with aging, a phenotype that is dependent on
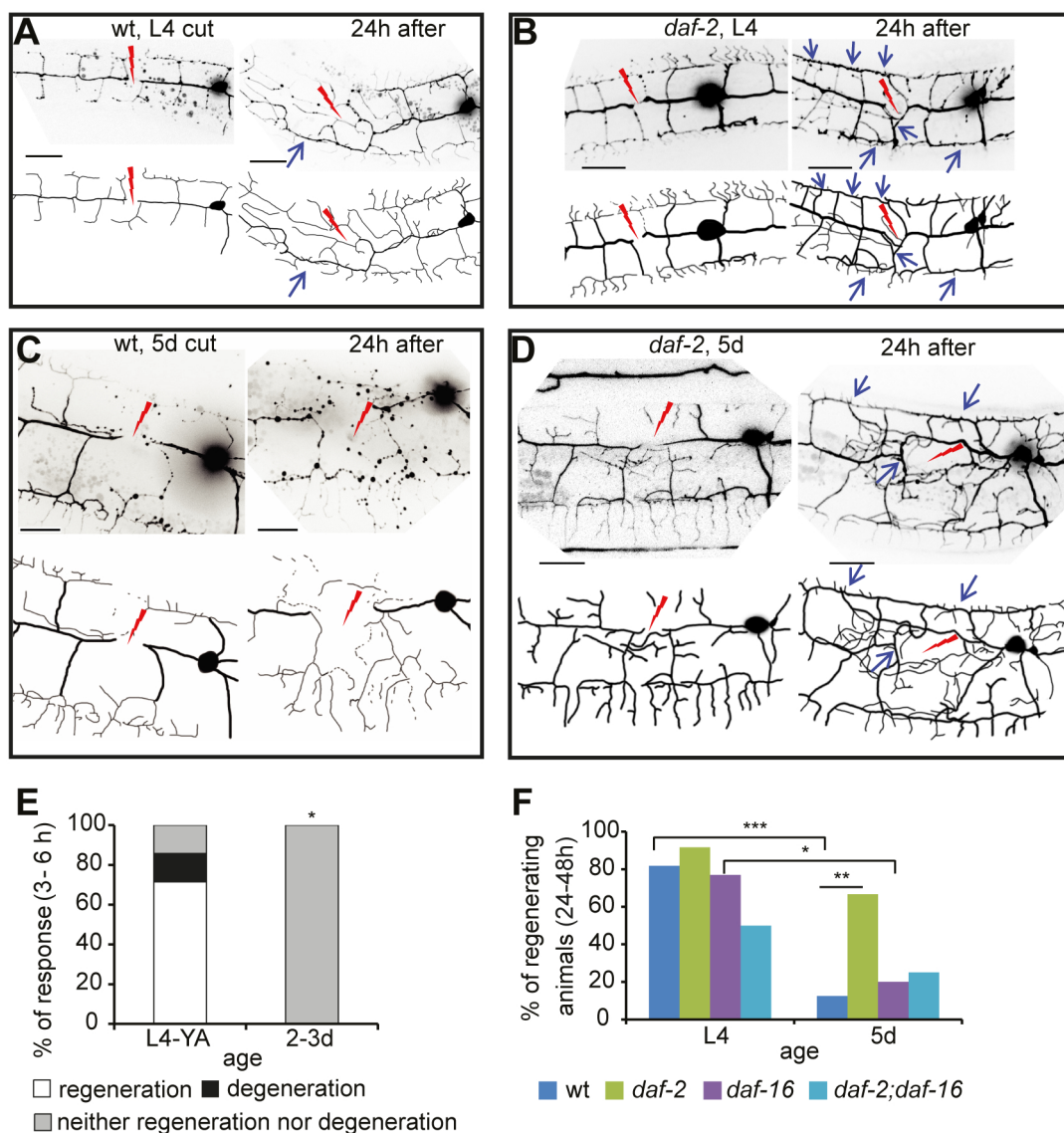
244   DAF-2/IGF-1R and its target DAF-16/FOXO.

245

246

Fig 5. *daf-2*(-) restores regenerative ability of aged animals via *daf-16*

248   **(A-D)** PVD neurons immediately after cut and 24 h later in wild-type and *daf-2* mutants at L4
249   and 5 days of adulthood (5d), as indicated. Schematic illustrations below negative images.
250   Red lightings, injury sites. Blue arrows, fusion sites (successful regeneration). Scale bars, 20
251   μm.

252 **(E)** Response to injury of wild-types at L4-young adult (YA) and 2-3d within a short time (3-
253 6 h) after injury. Number of animals: n=7 (L4 –YA) and n=4 (2-3d).

254 **(F)** Percentage of successfully regenerating animals within 24-48 h post injury. *p* values from
255 *Fisher's exact tests*: * *p<0.05*, ** *p<0.01*, *** *p<0.001*. Number of animals: n ≥ 8. See also
256 **Fig S3** and **Movies S2-S4**.

257

258 **AFF-1 mediates and restores dendrite regeneration in aged animals**

259 AFF-1 (Anchor cell Fusion Failure 1), is a transmembrane protein related to EFF-1 that

260 executes several cell-cell fusion events during development in the epidermis, excretory,

261 digestive and reproductive systems [39]. *aff-1* mutants have no evident morphological

262 phenotypes in the PVD neuron and its expression has not been detected in the PVD (**Fig S3**);

263 moreover, when AFF-1 is ectopically expressed in the PVD in an *eff-1* mutant background it

264 does not retract excess branching, demonstrating that it is unable to rescue the pruning

265 defects of *eff-1* **(Fig S4)**. This result shows that EFF-1 and AFF-1 fusion proteins have

266 different activities and are not interchangeable in the PVD neuron. However, AFF-1 is

267 required for dendrite fusion in response to injury in L4s and young adults [40]. Adults carrying

268 loss-of-function mutations in *aff-1* have severe egg laying defects, shorter life spans and

269 excretory system defects that prevented us from studying regeneration in aging *aff-1* mutant

270 animals. To investigate whether AFF-1 can restore the regenerative ability of dendrites in

271 older animals we overexpressed AFF-1 specifically in the PVD (PVDp::AFF-1; **Fig S5**). We

272 found that the structural units of young animals expressing PVDp::AFF-1 appeared

273 morphologically wild-type and responded similarly to dendrotomy **(Fig 6A, Movie S5)**.

274 However, when 5-day old PVDp::AFF-1 animals were dendrotomized, the percentage of

275 regenerating worms by dendrite fusion was significantly higher compared to wild-type

276 animals (60-80% and 13%, respectively; **Fig 6B and 6C, Movie S6)**. Thus, AFF-1-specific

277 overexpression in the PVD enables dendrite regeneration via auto-fusion of cut dendrites in

278 older animals **(Fig 6C)**. This autonomous and ectopic expression of the fusion protein AFF-1

279 in the PVD appears to rejuvenate the ability to reconnect cut dendrites by the self-fusion

13

280 mechanism. Since endogenous AFF-1 expression cannot be detected in the PVD ([40]; Fig. S3),

281 it appears that ectopic activity of the AFF-1 fusion protein in the PVD neuron is sufficient to

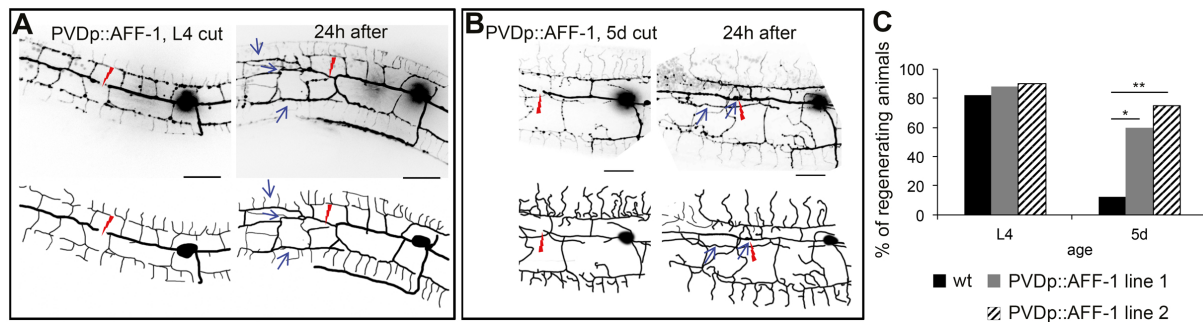282 repair and remodel severed dendrites via the mechanism of auto-fusion in middle aged adults.

283

Fig 6. AFF-1 enhances regeneration by dendrite fusion in 5d-old animals

(A-B) Inverted fluorescence images of PVD neurons immediately after cut and 24 hours (h) later in animals overexpressing AFF-1 in the PVD (PVDp::AFF-1), at L4 and 5 days of adulthood (5d), as indicated on each image (schematic drawings below each image). Red lightning marks the injury site and blue arrows point at dendrite fusion sites. Scale bars, 20 µm.

(C) Percentage of successfully regenerating animals within 24-48h after injury. *p* value from *Fisher's exact test*: * *P<0.05*; ** *P<0.001*. Number of animals: n ≥ 10. See also **Movies S5-S6**. PVDp::AFF-1 line 1 and 2 correspond to worms carrying the extrachromosomal arrays *hyEx390* and *hyEx391,* respectively.

296

Rejuvenation of fusion potential of cut dendrites by *daf-2(-)* and AFF-1(+)

298 We wished to further compare the regenerative modalities of AFF-1 overexpression and *daf-*

299 *2* mutation following dendritic laser-induced severing in aging animals. Dendritic fusion

300 following injury can occur by three possible pathways: 1) 3ry-3ry branch fusions that bypass

301 the injury site ("menorah-menorah" fusion); 2) fusion of the proximal primary (1ry) branch to

302 the detached distal 1ry; 3) both 3ry-3ry fusion and 1ry-1ry fusion **(Fig 7A)**. To determine

303 whether the mechanism of remodeling of dendritic trees following injury is distinct in wild-

304 type, *daf-2* reduced function mutants and in animals ectopically expressing AFF-1 in the

305 PVD, we compared the remodeling of dendritic trees in aging animals in these three

306   genotypes following injury. We found that in wild-type and PVDp::AFF-1 animals at the L4

307   stage, the most prevalent mechanism of repair is 3ry-3ry fusion (pathway 1), whereas in *daf-2*

308   mutants 3ry-3ry fusion together with 1ry-1ry fusion (pathway 3) increased compared to wild-

309   type **(Fig 7B-7D)**. In wild-type, we found degeneration in 50% (2-4d) and 80% (5-6d) of the

310   dendrotomized animals **(Fig 7E** and **7H)**. Adult *daf-2* mutant animals (5-6d) presented a

311   response to injury that resembled that observed in L4 wild-type animals, with 70% of the

312   animals showing regeneration, mainly via 3ry-3ry fusions **(Fig 7F** and **7I)**. In contrast, in

313   PVDp::AFF-1 animals the response to injury followed a different mechanism, with more

314   regeneration via enhanced 1ry-1ry fusion instead of 3ry-3ry fusion as observed in *daf-2*

315   mutants (Fig 7G and 7J). However, the AFF-1 effect was unrelated to longevity as

316   PVDp::AFF-1 animals had normal lifespans **(Fig S6)**. Thus, differential activities of AFF-

317   1(+) and *daf-2*(-) maintain the remodeling potential of aging arbors, and the mechanisms of

318   rejuvenation by fusion that prevent degeneration appear to be independent. In both cases

319   degeneration of the distal trees is prevented.

320   Aged dendritic trees lose their regenerative potential because following laser-induced

321   dendrotomy old neurons usually fail to auto-fuse broken dendrites and undergo degeneration.

322   DAF-2/ IGF-1R negatively regulates the regeneration process. When the fusogen AFF-1 is

323   ectopically expressed in the PVD neuron it has an anti-aging activity that promotes auto-

324   fusion of old transected primary dendrites.

325

Fig 7. *daf-2*(-) and AFF-1(+) rejuvenate fusion potential of broken dendrites

(A) Cartoon representing four possible outcomes of dendrotomy. Dendrite auto-fusion indicates successful regeneration (outcomes 1-3), if fusion does not occur degeneration takes place (outcome 4).

(B-J) Percentages of wild-type worms (wt), *daf-2* mutants and AFF-1 overexpressing animals (PVDp::AFF-1) at different ages, divided into the four different types of response to injury as described in **(A)**. Genotype and age are listed above each plot. *p* values from *Fisher's exact tests*: * *p<0.05*, ** *p<0.01*, *** *p<0.001*. Additional significant differences were found between: (**C** and **F**), (**C** and **I**) and between (**B** and **J**) (*p<0.05*).

Discussion

Precise dendritic arborization is critical for proper functioning of neuronal networks, while defective dendritic development and maintenance lead to neuropathologies [56,57]. There is evidence from mammalian CNS showing increase in number and length of terminal dendritic arbors during aging, and reduced arborization in senile dementia [58]. However, it remains unclear whether there is a direct link between altered dendritic structure and reduced function in mammals. Axons of aging neurons also show altered morphologies in diverse species. In *C. elegans* these axonal alterations are not affected by organismal longevity [11,51,52,59]. Here we also found that dendritic alterations during aging are not affected by chronological age; however, unlike the PVD dendrites, in axons the *daf-2* mutation was found to delay the morphological alterations of aged animals [8-10]. Nevertheless, the *daf-2* effect in age-related axonal branching was reported to be uncoupled of its role in extending the lifespan of the worms [8,9]. It thus appears that DAF-2 is specifically involved in cell-autonomous pathways that maintain axonal, but not dendritic morphology. We observed a small but significant decline in response to harsh touch during aging in both wild-type and *daf-2* (Fig. 4). Thus, we propose that the dendrite overgrowth observed in old animals reveal a reduction in morphological plasticity and a normal change in the architecture of the dendritic trees that do not appear to have major functional consequences in the ability to respond to noxious mechanosensory stimuli. However, the link between structure and function needs to be further investigated in future studies. While progressive age-related hyperbranching of the PVD arbors was independent of insulin/IGF-1 pathway, overexpression of EFF-1 in the PVD was sufficient to partially rescue this phenotype in old animals (**Fig S7**). EFF-1 appears to act cell-autonomously to simplify the dendritic trees via its pruning activity mediated by branch retraction [28].

17

363   We further found that dendrite regeneration following PVD dendrotomy decreases

364   with age. This decline was "rescued" in *daf-2* mutants (**Fig 5**). Axonal regeneration is

365   known to decline with age in different organisms [11,51,52,59-61]. In GABA neurons of *C. elegans*

366   the decline in axonal regeneration is also delayed in *daf-2* mutants [11]. However, these neurons

367   do not engage in self-fusion during regeneration, whereas in PVD dendrites the main

368   outcome of regeneration is auto-fusion. Recently, an important role of auto-fusion during

369   axonal regeneration was demonstrated in the PLM sensory neurons of *C. elegans*, a process

370   mediated by the fusogen EFF-1 [15,18]. In the PVD EFF-1 is not necessary for dendrite

371   reconnection following injury [40]. In the PVD dendrites, this role is fulfilled by the EFF-1

372   paralog AFF-1. Significantly, when AFF-1 is ectopically expressed, this fusogen plays a role

373   in maintenance of regenerative potential during aging (**Figs 7 and 8**). These findings

374   highlight fusion mechanisms as potential target for pharmacological intervention in

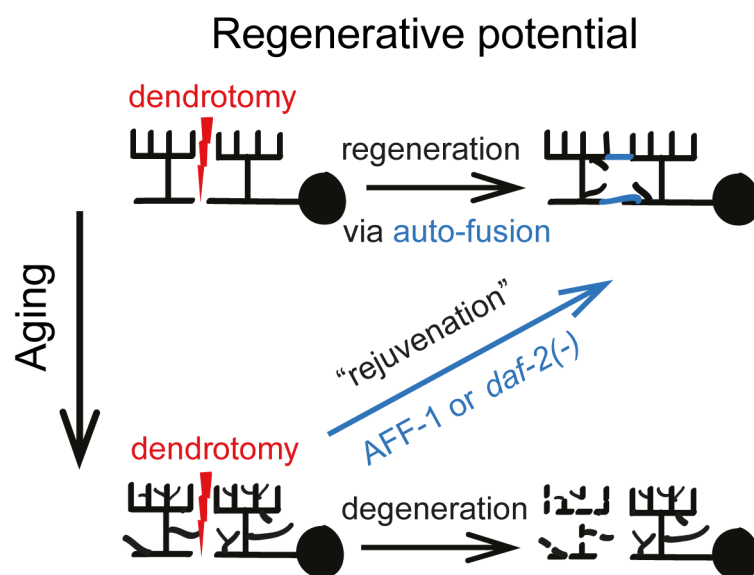375   neuropathologies that result from both injury and aging.

376

Fig 8. Model for rejuvenation of the regenerative potential of dendritic arbors
Aged multibranched neurons lose their ***regenerative potential*** because following laser-induced dendrotomy old PVDs usually fail to auto-fuse broken dendrites and undergo degeneration. DAF-2/ IGF-1R negatively regulates the regeneration process. When the fusogen AFF-1 is ectopically expressed in the PVD neuron it has an anti-aging activity that promotes auto-fusion of old transected primary dendrites.

383

384 **Materials and Methods**

385 **Nematode strains**

386 Animals were maintained at 20°C, unless otherwise stated, according to standard protocols [62].

387 All experiments were performed on hermaphrodites. N2 served as wild-type, and the

388 following mutants and transgenic strains were used:

389 NC1841 *[wdIs52(F49H12.4::GFP); rwIs1(pmec-7::RFP)]* [29], outcrossed 4X, CHB392

390 *[hmnEx133(ser-2prom3::kaede)],* kindly provided by Candice Yip and Max Heiman [63],

391 BP709 *[hmnIs133 (ser-2prom3::kaede)]*, kindly provided by Tamar Gattegno, MF190

392 *[hmIs4(des-2::gfp, pRF4)]* [28]. CB1338 *[mec-3(e1318)IV]*, *Caenorhabditis* Genetics Center

393 (CGC), CB1611 *[mec-4(e1611)X]*, (CGC), BP176 *[hyEx23(des-2::eff-1, des-2::gfp, pRF4)]*

394 [28], BP177 *[hyEx392(des-2::eff-1, des-2::gfp, pRF4)]*, BP488 *[eff-1(hy21)II; hmIs4;*

395 *hyEx39(des-2p::AFF-1,myo-2::GFP,KS)]*, BP906 *[daf-2(e1370)III; wdIs52; rwIs1],* BP911

396 *[hyEx39; hmnEx133]*, BP915 *[hyEx39; hmnIs133]*, BP551 *[hyEx391(des-2p::AFF-1, myo-*

397 *2::GFP, KS); hmnEx133],* BP919 *[daf-2(e1370)III; daf-16(mu86)I; hmnIs133],* BP923

398 *[daf-16(mu86)I; hmnIs133]*, BP924 *[daf-2(e1370)III; hmnIs133]*, BP925 *[mec-4(e1611)X;*

399 *hmnIs133]*, BP926 *[daf-2(e1370)III;mec-4(e1611)X; hmnIs133]*, BP1056 *hyEx68[AFF-*

400 *1::TY1::EGFP::3xFLAG, pRF4, KS]; dzIs53[F49H12.4p:mCherry], AFF-*

401 *1::TY1::EGFP::3xFLAG* was kindly provided by transgenome project [64], BP500 *zzIs22*

402 *[pJdC41(eff-1p::EFF-1::GFP), pRF4]; dzIs53 (pF49H12.4::mCherry) zzIs22* was kindly

403 provided by William Mohler [65].

404 **Molecular Biology**

405 The *ser-2prom3::Kaede* (pCY2 plasmid) is a kind gift from Candice Yip and Max Heiman [63].

406 It was constructed by digesting *ser-2prom3* with SbfI and AscI and Kaede with AscI and

407 NotI and then ligated together.

408   The *des-2p::AFF-1* construct (pME4 plasmid) was constructed by inserting an AFF-1

409   genomic fragment, digested from *hsp16.2::AFF-1* [39] with NheI and KpnI and cloned into

410   pME2 [28] cut with the same enzymes. *des-2p::AFF-1* was injected at a concentration of 0.1ng/ml

411   into *eff-1(hy21)* animals and three independent lines were obtained. For dendrotomy experiments,

412   two lines (*hyEx39* and *hyEx391*) were crossed into a wild-type background expressing the PVD

413   marker *ser-2p3::Kaede.*

414   **Live imaging of worms**

415   Time-lapse imaging and short imaging (one time point) of worms by Nomarski optics and

416   fluorescence microscopy was performed using a Nikon eclipse Ti inverted microscope with

417   Yokogawa CSU-X1 spinning disk or using the Zeiss Laser Scanning Microscope (LSM) 510

418   META. Animals were anesthetized using 0.1% tricaine and 0.01% tetramisole in M9

419   solution for 20-30 minutes, and then they were transferred to a 3% agar slide with an eyelash

420   attached to a toothpick. For short time imaging worms were often mounted on 3% agar slides

421   containing 5–10 mM NaN_3 instead. Image acquisition was done using Andor iQ or

422   Metamorph software, when using the spinning disk confocal (SDC), and Zen software when

423   using the LSM 510 meta microscope. Z-stacks were taken with PlanApochromat 60x oil

424   NA=1.4 objective using the SDC or 63x NA=1.4 objective using the LSM. Excitation of

425   GFP and green Kaede was done with 488 nm wavelength laser and 525 filter (6-15%, 50 ms

426   exposure time), RFP and red Kaede was excited with 561 nm wavelength laser and 607 filter

427   (15-20%, 50-100 ms exposure time). When using the sCMOS (Andor) camera z-stacks were

428   taken with ~0.23 μm z-step. With iXon EMCCD camera (Andor) z-stacks were taken with

429   ~0.5 μm z- step, gain was ~100. When the LSM 510 meta was used, z-step was ~0.8 μm.

430   Multidimensional data was reconstructed as maximum intensity projections using the FIJI

431   software (NIH Image). Images were prepared using Imaris, FIJI and Adobe Photoshop CS5.

432   Final figures were constructed using Adobe Illustrator CS5.1.

Laser dendrotomies

Micropoint, pulsed nitrogen laser, or the tunable Chameleon Ultra Ti-Sapphire laser system (two-photon), were used to sever the primary dendrite of the PVD. The Micropoint system was used on the Nikon eclipse Ti inverted microscope with Yokogawa CSU-X1 spinning disk. In order to transect neurons, we used 405 beamsplitter and 365nm dye cell and either IQ or Metamorph software. We used highest levels with the attenuator plate (all the way in), while the software controlled attenuator was adjusted between 80-90% when using IQ, and 30-50% when using Metamorph. Roughly 15 pulses at 10 Hz were administered for each cut in IQ and Metamorph. For all worms the primary dendrite was injured anterior to cell body. Animals were imaged and a z-stack was collected immediately after cut to confirm that the injury was successful.

The two-photon system was used on the Zeiss LSM 510 META microscope. The laser produces 200fs short pulses at 113MHz repetition rate and energy of 5nJ. In order to cut neurons we used 820 nm wavelength and 20-30% laser power using the Zen software. Worms were imaged immediately after cut to confirm that the injury was successful, and z-stacks were taken using the spinning disk confocal system or the LSM 510 META as described for live imaging of worms. After surgery, animals were recovered on NGM agar plates seeded with OP50 in a drop of M9 and imaged again later, or time-lapse movies were immediately acquired.

Regeneration was defined as continuation of the fluorescent signal between the distal and proximal ends or using Kaede photoconversion (**Fig S3**; see below). Significant differences between ages and genotypes were determined using *Fisher's exact test*.

Kaede photoconversion

In order to verify that dendrites fuse as response to injury we used the photoconvertible protein Kaede driven by a PVD specific promoter *ser-2prom3* [63]. Irreversible

458   photoconversion of the green Kaede to red Kaede was achieved using Mosaic system on the

459   Nikon eclipse Ti inverted microscope with Yokogawa CSU-X1 spinning disk, at 405 nm, 20-

460   50 ms exposure time with 10-20 repeats across the region of interest, which was always the

461   cell body, using either IQ or Metamorph software.

Morphological quantitation of the PVD

463   Branch count and disorganization of PVD structural units (menorahs) was counted in the 100

464   μm around cell body (unless otherwise stated), as previously described [28]. Lack of self-

465   avoidance between adjacent menorahs was determined in the same region as previously

466   described [46]. Z-stack maximum intensity projections of time-lapse movies were analyzed

467   manually, using FIJI software. Factorial analysis of variance (ANOVA) and *t-tests* were

468   performed to compare between genotypes and ages.

Harsh touch assay

470   Harsh touch assay was performed as previously described [28,50] and the experimenter was

471   blind to the genotype. The experiments were done in light touch mutant background (*mec-*

472   *4(e1611)*) [66]. *mec-3(e1338)* worms were used as negative control [50]. Significant differences

473   between the ages were determined by the $\chi 2$ test.

Life-span assay

475   Lifespan assays were carried out at 20°C as previously described [67]. A population of worms

476   was synchronized using hypochlorite and NaOH solution and ~100 animals at the L4

477   "Christmas tree" stage were placed on NGM plates containing 49.5 μM 5-Fluoro-2′-

478   deoxyuridine (FUDR, Sigma, F0503) seeded with OP50 *E. coli*, at a density of 20 worms per

479   6 cm plate. Adult day 1 was designated as the day after the L4 larval stage that served as

480   time 0. Animals were scored as dead or alive every 2-3 days until all animals died. An

481   animal was scored dead when it did not move or react at all to prodding with a platinum wire.

482   Animals that crawled off of the plate, were trapped in fungal infection, "exploded" (i.e.,

483   showed extruded tissue from the vulva), or showed internal hatching ("bagging"), were

484   excluded. If plates were contaminated, animals were transferred to fresh plates, using

485   platinum wire. Statistical significance was determined using the Log-Rank (Mantel-Cox)

486   test.

487   **RNA Isolation, Reverse Transcription, and Quantitative Real-Time PCR.**

488   Total RNA from Wild-type worms and des-2p::AFF-1 transgenic worms was isolated using

489   the RNeasy Micro kit following the manufacturer's protocol (Qiagen). RNA was used for

490   cDNA synthesis using the qScript cDNA Synthesis Kit (Quanta BioSciences) with random

491   primers. Real-time PCR was performed using AFF-1 and Fast SYBR® Green Master Mix

492   (Applied Biosystems). The PCR amplification conditions were as follows: 40 cycles of 95 °C

493   for 20 s and 60 °C for 20 s. Each PCR was run in triplicate. Data analysis and quantification

494   were performed using StepOne software V2.2 supplied by Applied Biosystems. To account

495   for the variability in the initial concentration of the RNA, results were normalized to the

496   ACT-1 housekeeping gene.

497   **Statistical analysis**

498   Statistical analysis was performed using the GraphPad online tool:

499   http://www.graphpad.com/quickcalcs/ for *t-tests, Fisher's exact test*s and χ^2 tests. Analysis of

500   variance (ANOVA) that was performed when more than two groups were compared and Log-

501   Rank survival test, using SPSS. *Freeman-Halton* extension of the *Fisher's exact test* (for 2x4

502   contingency table) was performed using the Vassarstats.net online tool, to compare between

503   the distributions of response to injury between different genotypes and ages.

504   **Acknowledgments**

508   the Podbilewicz laboratory for discussion. Some strains were provided by the CGC, which is

509   funded by NIH Office of Research Infrastructure Programs (P40 OD010440).

510   **Author contributions:** VK, MOS and BP designed the experiments. VK performed most

511   experiments. MOS developed the system to study neuronal degeneration and regeneration

512   following dendrotomy using the PVD neurons. MOS generated the PVDp::AFF-1 and

513   PVDp::EFF-1 transgenics and MOS and VK tested the effects of EFF-1 and AFF-1 over-

514   expression on regenerating animals. BP supervised this work. VK, MOS and BP wrote the

515   paper.

516   The authors declare no conflict of interest.

517   This article contains supporting information including seven figures and six movies

518

519   **References**

520   1   Yankner, B. A., Lu, T. & Loerch, P. in *Annual Review of Pathology-Mechanisms of Disease* Vol. 3
521   *Annual Review of Pathology-Mechanisms of Disease*   41-66 (Annual Reviews, 2008).
522   2   Kenyon, C. J. The genetics of ageing. *Nature* **464**, 504-512, doi:10.1038/nature08980 (2010).
523   3   Hammarlund, M. & Jin, Y. Axon regeneration in C. elegans. *Current Opinion in Neurobiology* **27**,
524   199-207, doi:10.1016/j.conb.2014.04.001 (2014).
525   4   Ghosh-Roy, A. & Chisholm, A. D. Caenorhabditis elegans: A new model organism for studies of axon
526   regeneration. *Developmental Dynamics* **239**, 1460-1464, doi:10.1002/dvdy.22253 (2010).
527   5   Kenyon, C., Chang, J., Gensch, E., Rudner, A. & Tabtiang, R. A C-elegans mutant the lives twice as
528   long as wild- type *Nature* **366**, 461-464, doi:10.1038/366461a0 (1993).
529   6   Lin, K., Hsin, H., Libina, N. & Kenyon, C. Regulation of the Caenorhabditis elegans longevity protein
530   DAF-16 by insulin/IGF-1 and germline signaling. *Nature Genetics* **28**, 139-145, doi:10.1038/88850
531   (2001).
532   7   Murphy, C. T. *et al.* Genes that act downstream of DAF-16 to influence the lifespan of Caenorhabditis
533   elegans. *Nature* **424**, 277-284, doi:10.1038/nature01789 (2003).
534   8   Tank, E. M. H., Rodgers, K. E. & Kenyon, C. Spontaneous age-related neurite branching in
535   Caenorhabditis elegans. *J. Neurosci.* **31**, 9279-9288, doi:10.1523/jneurosci.6606-10.2011 (2011).
536   9   Toth, M. L. *et al.* Neurite sprouting and synapse deterioration in the aging Caenorhabditis elegans
537   nervous system. *J. Neurosci.* **32**, 8778-8790, doi:10.1523/jneurosci.1494-11.2012 (2012).
538   10   Pan, C.-L., Peng, C.-Y., Chen, C.-H. & McIntire, S. Genetic analysis of age-dependent defects of the
539   Caenorhabditis elegans touch receptor neurons. *Proc. Natl. Acad. Sci. U.S.A.* **108**, 9274-9279,
540   doi:10.1073/pnas.1011711108 (2011).
541   11   Byrne, A. B. *et al.* Insulin/IGF1 signaling inhibits age-dependent axon regeneration. *Neuron* **81**, 561-
542   573, doi:10.1016/j.neuron.2013.11.019 (2014).
543   12   Park, K. K. *et al.* Promoting axon regeneration in the adult CNS by modulation of the PTEN/mTOR
544   pathway. *Science* **322**, 963-966 (2008).
545   13   Taylor, A. M. *et al.* A microfluidic culture platform for CNS axonal injury, regeneration and transport.
546   *Nat Methods* **2**, 599-605, doi:nmeth777 [pii] 10.1038/nmeth777 (2005).
547   14   Ruschel, J. *et al.* Axonal regeneration. Systemic administration of epothilone B promotes axon
548   regeneration after spinal cord injury. *Science* **348**, 347-352, doi:10.1126/science.aaa2958 (2015).
549   15   Neumann, B. *et al.* EFF-1-mediated regenerative axonal fusion requires components of the apoptotic
550   pathway. *Nature* **517**, 219-U259, doi:10.1038/nature14102 (2015).

16   Neumann, B., Nguyen, K. C. Q., Hall, D. H., Ben-Yakar, A. & Hilliard, M. A. Axonal Regeneration Proceeds Through Specific Axonal Fusion in Transected C. elegans Neurons. *Developmental Dynamics* **240**, 1365-1372, doi:10.1002/dvdy.22606 (2011).

17   Hoy, R. R., Bittner, G. D. & Kennedy, D. Regeneration in Crustacean motoneurons - evidence for axonal fusion *Science* **156**, 251-&, doi:10.1126/science.156.3772.251 (1967).

18   Ghosh-Roy, A., Wu, Z. L., Goncharov, A., Jin, Y. S. & Chisholm, A. D. Calcium and cyclic AMP promote axonal regeneration in Caenorhabditis elegans and require DLK-1 kinase. *J. Neurosci.* **30**, 3175-3183, doi:10.1523/jneurosci.5464-09.2010 (2010).

19   Paltsyn, A., Komissarova, S., Dubrovin, I. & Kubatiev, A. Increased cell fusion in cerebral cortex may contribute to poststroke regeneration. *Stroke research and treatment* **2013**, 869327-869327, doi:10.1155/2013/869327 (2013).

20   Alvarez-Dolado, M. *et al.* Fusion of bone-marrow-derived cells with Purkinje neurons, cardiomyocytes and hepatocytes. *Nature* **425**, 968-973, doi:http://www.nature.com/nature/journal/v425/n6961/suppinfo/nature02069_S1.html (2003).

21   Johansson, C. B. *et al.* Extensive fusion of haematopoietic cells with Purkinje neurons in response to chronic inflammation. *Nature Cell Biology* **10**, 575-583, doi:10.1038/ncb1720 (2008).

22   Giordano-Santini, R., Linton, C. & Hilliard, M. A. Cell-cell fusion in the nervous system: Alternative mechanisms of development, injury, and repair. *Seminars in cell & developmental biology*, doi:10.1016/j.semcdb.2016.06.019 (2016).

23   Mohler, W. A. *et al.* The type I membrane protein EFF-1 is essential for developmental cell fusion in *C. elegans*. *Dev Cell* **2**, 355-362 (2002).

24   Podbilewicz, B. *et al.* The C. elegans developmental fusogen EFF-1 mediates homotypic fusion in heterologous cells and in vivo. *Dev Cell* **11**, 471-481 (2006).

25   Shemer, G. *et al.* EFF-1 is sufficient to initiate and execute tissue-specific cell fusion in *C. elegans*. *Curr Biol* **14**, 1587-1591 (2004).

26   Pérez-Vargas, J. *et al.* Structural basis of eukaryotic cell-cell fusion. *Cell* **157**, 407-419 (2014).

27   Tsalik, E. L. *et al.* LIM homeobox gene-dependent expression of biogenic amine receptors in restricted regions of the C-elegans nervous system. *Developmental Biology* **263**, 81-102, doi:10.1016/s0012-1606(03)00447-0 (2003).

28   Oren-Suissa, M., Hall, D. H., Treinin, M., Shemer, G. & Podbilewicz, B. The fusogen EFF-1 controls sculpting of mechanosensory dendrites. *Science* **328**, 1285-1288, doi:10.1126/science.1189095 (2010).

29   Smith, C. J. *et al.* Time-lapse imaging and cell-specific expression profiling reveal dynamic branching and molecular determinants of a multi-dendritic nociceptor in C. elegans. *Dev. Biol.* **345**, 18-33, doi:10.1016/j.ydbio.2010.05.502 (2010).

30   Chatzigeorgiou, M. *et al.* Specific roles for DEG/ENaC and TRP channels in touch and thermosensation in C. elegans nociceptors. *Nat. Neurosci.* **13**, 861-U106, doi:10.1038/nn.2581 (2010).

31   Salzberg, Y. *et al.* Skin-derived cues control arborization of sensory dendrites in Caenorhabditis elegans. *Cell* **155**, 308-320, doi:10.1016/j.cell.2013.08.058 (2013).

32   Dong, X., Liu, O. W., Howell, A. S. & Shen, K. An extracellular adhesion molecule complex patterns dendritic branching and morphogenesis. *Cell* **155**, 296-307, doi:10.1016/j.cell.2013.08.059 (2013).

33   Dong, X., Shen, K. & Bülow, H. E. Intrinsic and Extrinsic Mechanisms of Dendritic Morphogenesis. *Annual Review of Physiology* **77**, null, doi:doi:10.1146/annurev-physiol-021014-071746 (2015).

34   Liu, O. W. & Shen, K. The transmembrane LRR protein DMA-1 promotes dendrite branching and growth in C. elegans. *Nat. Neurosci.* **15**, 57-U74, doi:10.1038/nn.2978 (2012).

35   Maniar, T. A. *et al.* UNC-33 (CRMP) and ankyrin organize microtubules and localize kinesin to polarize axon-dendrite sorting. *Nat. Neurosci.* **15**, 48-U66, doi:10.1038/nn.2970 (2012).

36   Cohen, E. *et al.* Caenorhabditis elegans nicotinic acetylcholine receptors are required for nociception. *Molecular and Cellular Neuroscience* **59**, 85-96, doi:10.1016/j.mcn.2014.02.001 (2014).

37   Husson, S. J. *et al.* Optogenetic Analysis of a Nociceptor Neuron and Network Reveals Ion Channels Acting Downstream of Primary Sensors. *Current Biology* **22**, 743-752, doi:10.1016/j.cub.2012.02.066 (2012).

38   Wei, X. *et al.* The unfolded protein response is required for dendrite morphogenesis. *eLife* **4**, e06963, doi:10.7554/eLife.06963 (2015).

39   Sapir, A. *et al.* AFF-1, a FOS-1-regulated fusogen, mediates fusion of the anchor cell in C-elegans. *Dev. Cell* **12**, 683-698, doi:10.1016/j.devcel.2007.03.003 (2007).

40   Oren-Suissa, M., Gattegno, T., Kravtsov, V. & Podbilewicz, B. Extrinsic repair of injured dendrites as a paradigm for regeneration by fusion. *Preprint. Available: BioRxiv*, doi:http://dx.doi.org/10.1101/062372 (2016).

41   Procko, C., Lu, Y. & Shaham, S. Glia delimit shape changes of sensory neuron receptive endings in C. elegans. *Development* **138**, 1371-1381, doi:10.1242/dev.058305 (2011).

42   Stone, C. E., Hall, D. H. & Sundaram, M. V. Lipocalin signaling controls unicellular tube development in the Caenorhabditis elegans excretory system. *Dev Biol* **329**, 201-211, doi:10.1016/j.ydbio.2009.02.030 (2009).

43   Rasmussen, J. P., English, K., Tenlen, J. R. & Priess, J. R. Notch signaling and morphogenesis of single-cell tubes in the C. elegans digestive tract. *Dev Cell* **14**, 559-569 (2008).

44   Soulavie, F. & Sundaram, M. V. Auto-fusion and the shaping of neurons and tubes. *Seminars in cell & developmental biology*, doi:10.1016/j.semcdb.2016.07.018 (2016).

45   Lenard, A. *et al.* Endothelial cell self-fusion during vascular pruning. *PLoS biology* **13**, e1002126-e1002126, doi:10.1371/journal.pbio.1002126 (2015).

46   Smith, C. J., Watson, J. D., VanHovene, M. K., Colon-Ramos, D. A. & Miller, D. M., III. Netrin (UNC-6) mediates dendritic self-avoidance. *Nat. Neurosci.* **15**, 731-737, doi:10.1038/nn.3065 (2012).

47   Oren-Suissa, M., Hall, D., Treinin, M., Shemer, G. & Podbilewicz, B. The Fusogen EFF-1 Controls Sculpting of Mechanosensory Dendrites. *Science* **328**, 1285-1288, doi:10.1126/science.1189095 (2010).

48   Smith, C. J., Watson, J. D., VanHoven, M. K., Colon-Ramos, D. A. & Miller, D. M., 3rd. Netrin (UNC-6) mediates dendritic self-avoidance. *Nat Neurosci* **15**, 731-737, doi:10.1038/nn.3065 (2012).

49   Smith, C. J. *et al.* Time-lapse imaging and cell-specific expression profiling reveal dynamic branching and molecular determinants of a multi-dendritic nociceptor in C. elegans. *Dev Biol* **345**, 18-33, doi:S0012-1606(10)00805-5 [pii] 10.1016/j.ydbio.2010.05.502 (2010).

50   Way, J. C. & Chalfie, M. The mec-3 gene of Caenorhabditis-elegans requires its own product for maintained expression and is expressed in 3 neuronal cell-types *Genes Dev.* **3**, 1823-1833, doi:10.1101/gad.3.12a.1823 (1989).

51   Verdu, E., Ceballos, D., Vilches, J. J. & Navarro, X. Influence of aging on peripheral nerve function and regeneration. *J. Periph. Nerv. Syst.* **5**, 191-208, doi:10.1046/j.1529-8027.2000.00026.x (2000).

52   Zou, Y. *et al.* Developmental decline in neuronal regeneration by the progressive change of two intrinsic timers. *Science* **340**, 372-376, doi:10.1126/science.1231321 (2013).

53   Bekkers, J. M. & Hausser, M. Targeted dendrotomy reveals active and passive contributions of the dendritic tree to synaptic integration and neuronal output. *Proc Natl Acad Sci U S A* **104**, 11447-11452, doi:0701586104 [pii] 10.1073/pnas.0701586104 (2007).

54   Rao, K. *et al.* Spastin, atlastin, and ER relocalization are involved in axon but not dendrite regeneration. *Mol Biol Cell* **27**, 3245-3256, doi:10.1091/mbc.E16-05-0287 (2016).

55   Nawabi, H., Zukor, K. & He, Z. No simpler than mammals: axon and dendrite regeneration in Drosophila. *Genes Dev* **26**, 1509-1514, doi:10.1101/gad.198150.112 (2012).

56   Jan, Y. N. & Jan, L. Y. Branching out: mechanisms of dendritic arborization. *Nat. Rev. Neurosci.* **11**, 316-328, doi:10.1038/nrn2836 (2010).

57   Koleske, A. J. Molecular mechanisms of dendrite stability. *Nat. Rev. Neurosci.* **14**, 536-550, doi:10.1038/nrn3486 (2013).

58   Buell, S. J. & Coleman, P. D. Dendritic growth in the aged human-brain and failure of growth in senile dementia *Science* **206**, 854-856, doi:10.1126/science.493989 (1979).

59   Hammarlund, M., Nix, P., Hauth, L., Jorgensen, E. M. & Bastiani, M. Axon regeneration requires a conserved MAP kinase pathway. *Science* **323**, 802-806, doi:10.1126/science.1165527 (2009).

60   Gabel, C. V., Antonie, F., Chuang, C.-F., Samuel, A. D. T. & Chang, C. Distinct cellular and molecular mechanisms mediate initial axon development and adult-stage axon regeneration in C. elegans. *Development* **135**, 1129-1136, doi:10.1242/dev.013995 (2008).

61   Pestronk, A., Drachman, D. B. & Griffin, J. W. Effects of aging on nerve sprouting and regeneration *Exp. Neurol.* **70**, 65-82, doi:10.1016/0014-4886(80)90006-0 (1980).

62   Brenner, S. Genetics of Caenorhabditis-elegans *Genetics* **77**, 71-94 (1974).

63   Yip, Z. C. & Heiman, M. G. Duplication of a Single Neuron in C. elegans Reveals a Pathway for Dendrite Tiling by Mutual Repulsion. *Cell reports*, doi:10.1016/j.celrep.2016.05.003 (2016).

64   Sarov, M. *et al.* A recombineering pipeline for functional genomics applied to Caenorhabditis elegans. *Nat Methods* **3**, 839-844, doi:10.1038/nmeth933 (2006).

65   del Campo, J. J. *et al.* Fusogenic activity of EFF-1 is regulated via dynamic localization in fusing somatic cells of C. elegans. *Curr Biol* **15**, 413-423 (2005).

66   Chalfie, M. & Sulston, J. Developmental genetics of the mechanosensory neurons of Caenorhabditis-elegans *Dev. Biol.* **82**, 358-370, doi:10.1016/0012-1606(81)90459-0 (1981).

67   Apfeld, J. & Kenyon, C. Cell nonautonomy of C-elegans daf-2 function in the regulation of diapause and life span. *Cell* **95**, 199-210, doi:10.1016/s0092-8674(00)81751-1 (1998).